MISSIONE 4
ISTRUZIONE
RICERCA

Hydrothermal versus microbial MEthane release From very shallow coastal systems: can differently sourced emISsions direcTly escape intO the atmosphere? (MEFISTO)

Deliverable 7. Conceptual and quantitative CH_4 emission models - *Final Report of the activities related to WP5*

Semprebello A., Bazzaro M., Caruso C., De Rosa G., De Vittor C., Esposito. V., Fonti V., Graziano M., Iacuzzo F., Longo M., Lazzaro G.

Finanziato dall'Unione europea NextGenerationEU | Ministero dell'Università e della Ricerca | Italiadomani PIANO NAZIONALE DI RIPRESA E RESILIENZA | OGS Istituto Nazionale di Oceanografia e di Geofisica Sperimentale

MISSIONE 4
ISTRUZIONE
RICERCA

Table of Content

1. SUMMARY

Following the pre-surveys of the seepage zone off the Marano and Grado lagoon (Northern Adriatic Sea) and the hydrothermal vent area off the Panarea island (Southern Tyrrhenian Sea), which have been accurately described in Deliverables 1-3, this report summarises the field and post-processing activities carried out within the framework of the MEFISTO project to develop specific algorithms aimed at the recognition of the noise produced from ascending bubbles and the following identification of degassing patterns and estimation methane gas released at six different sites located in these two shallow Italian coastal systems.
In addition, preliminary results about the different diffusion styles and quantification estimated on the various examined matrices are presented.
The collected data will help to shed light on the dynamics influencing the gaseous emissions from shallow near-shore marine environments by ascertaining possible differences in the water column degassing pathways and fates between microbially sourced and volcanic-related methane emissions. This, in turn, will lead to the achievement of the main goal of the MEFISTO project: to help define the actual contribution of coastal areas to global atmospheric methane, which remains subject to significant uncertainties.

MEFISTO research party during the pre-survey and first sampling campaign in the hydrothermal vent area off Panarea Island (March 20-23, 2024).

2. MEFISTO RESEARCH PROGRAMME AND OBJECTIVES

2.1 General scientific background

Methane (CH_4), accounting for about 30% of the ongoing atmospheric warming, is today recognized as one of the most powerful greenhouse gases (GHGs), being an even stronger absorber of Earth's emitted thermal infrared radiation than carbon dioxide (Simson, 2021). Atmospheric CH_4 concentrations, which increased by only 700 ppb during the millennium before industrialization, are now more than 2.6 times above estimated pre-industrial equilibrium levels, reaching 1857 ppb in 2018 (Saunois et al., 2020). Such an increase is largely the result of anthropogenic emissions related to human activities, including agriculture, production and utilisation of fossil fuel and waste management practices (Ciais et al., 2014). Nevertheless, since the lifetime of CH_4 in the atmosphere barely exceeds 10 years (Prather et al., 2012), the concentrations and therefore the radiative forcing of this potent GHG are thought to be scaled down in a few decades by just stabilising or reducing the anthropogenic emissions (Shindell et al., 2012). Such an approach is considered an effective and realistic way to rapidly mitigate climate change, making it possible to limit the global temperature rise to 1.5-2.0 °C, as targeted by the Paris Agreement (Nisbet et al., 2019).
In order to verify future emission reductions, a precise quantification of the global CH_4 budget is actually needed but, according to the most recent modelling, important uncertainties still affect the calculations, since global emissions were estimated to range between 576 Tg CH_4 / yr and 737 Tg CH_4 / yr (Saunois et al., 2020). The most important source of uncertainty is attributable to natural emissions, accounting for 40% of the global CH4 budget, 1-13% of which is due to the oceans (Kirschke et al., 2013; Saunois et al., 2016). However, while the open ocean CH_4 emissions are relatively well constrained and are driven by variations that are steadily linked to the organic matter cycling, the global marine flux appears to be mostly influenced by shallow near-shore environments (0-50 mbsl), where CH_4 released from the seafloor can escape to the atmosphere before oxidation (Weber et al., 2019). Here, many forcings can severely affect the amount of CH_4 that reaches the air-sea interface, above all water depth, currents, tides, temperature, water column stratification and microbial methane oxidation (Boles and Clark, 2001; Jordan et al., 2022; Mc Ginnis et al., 2006), but due to limited and few data, the actual contribution of coastal areas to atmospheric CH_4 is still quite uncertain (Weber et al., 2019).

2.2 The MEFISTO project

The MEFISTO project aims to reduce the abovementioned uncertainties in the estimates of the natural CH_4 fluxes by providing new data on the emissions from shallow near-shore marine environments, where, rapidly bypassing the water column by bubble transport, this powerful GHG can be directly released into the atmosphere (Weber et al., 2019). The lack of data on CH_4 fluxes in coastal areas has

significant implications for the accurate calculation of the atmospheric budget for this gas and the accuracy of this estimate is crucial for the verification of potential emissions reductions associated with the adoption of effective climate change mitigation strategies. The MEFISTO project, combining classical physical, chemical, and molecular methods with innovative hydroacoustic approaches, will help to fill this knowledge gap by focusing on the study of two Italian shallow coastal areas: a seepage zone recently identified in the Gulf of Trieste, centred on the Bardelli outcrop (Northern Adriatic Sea) and the hydrothermal vent area off the Panarea Island (Aeolian Archipelago, Southern Tyrrhenian Sea).

The project has three main purposes: 1) to ascertain possible differences in the water column degassing pathways and fates between microbially sourced and volcanic-related CH_4 emissions; 2) to assess the main physical and biological forcings (i.e., water depth, currents, tides, temperature, water column stratification and microbial community structure and composition) favouring or preventing the release of CH_4 to the atmosphere from the two investigated marine shallow areas; 3) to eventually develop local emission estimates that will contribute to the refinement of the global atmospheric CH_4 budget.

2.3 Volcanic-related CH_4 emissions: the hydrothermal vent system off the Panarea Island (Aeolian Archipelago, Southern Tyrrhenian Sea)

The Aeolian Archipelago is the expression of the volcanism migrating south-eastward from the Central and Southern Tyrrhenian Sea during the Lower Pleistocene and submarine emissions of CO_2-rich gases and thermal water discharges are documented in this area since the Roman Age (De Astis et al., 2003). The archipelago includes the active volcanoes of Stromboli, Vulcano, Lipari and Salina. Panarea is the smallest among the Aeolian Islands and represents the subaerial portion of a 2000 m high and 20 km wide submarine stratovolcano, a dormant edifice with a known age range of ca. 150-200 ka (Anzidei et al., 2005; Calanchi et al., 1999; Dolfi et al., 2007).

As a matter of fact, Panarea volcano was generally considered extinct until November 3, 2002, when a low-energy submarine explosion, due to the injection of magmatic fluids in the deep geothermal body (Caracusi et al., 2005), caused an intense and long-lasting submarine gas eruption in the ~2.3 km^2 area rimmed by the islets of Lisca Bianca, Bottaro, Lisca Nera, Dattilo, and Panarelli, about 2.5 km east of Panarea, leading to the opening of a submarine crater 20x8 m wide and 9 m deep (Anzidei and Esposito, 2003; Anzidei et al. 2005; Esposito et al. 2006; Figure 2.1).

The explosion released a huge amount of CO_2 that provoked a drop of seawater pH to a value of 5.6-5.7, killing all the living matter around the area, while the “degassing crisis” lasted several months (Caracusi et al., 2005; Romano et al., 2019).

Several studies conducted in the islet area indicated that, with about 98% CO_2, the composition of the persistent gaseous emissions is quite stable (Beaubien et al., 2014; Caliro et al., 2004; Espa et al., 2010; Marchini et al., 2021; Sani et al., 2024). Nevertheless, CH_4 concentrations, displaying values up to 900 ppm, are generally not negligible (Romano et al., 2019), making the islet area of Panarea suitable for the MEFISTO project purposes.

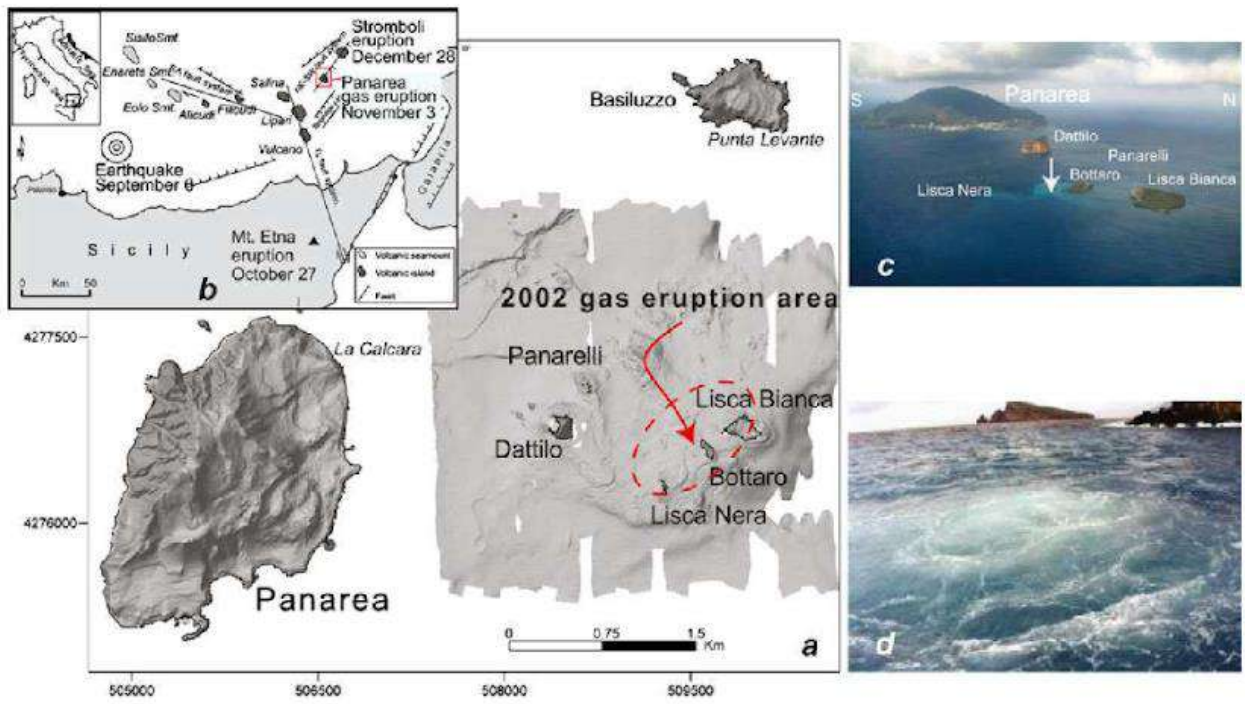

Figure 2.1. a) Location of the 2002 gas eruption. b) Structural sketch map of the Southern Tyrrhenian Sea and Aeolian Islands. c) Aerial view of Panarea Island and islet area with indication of major emission point. d) Gas bubbling in sea surface above the Bottaro crater. From Esposito et al. (2010).

2.4 Grébeni/Trezze/Tegnúe: methane-derived deposits in the Northern Adriatic Sea

The Northern Adriatic Sea is generally characterized by a rather monotonous seabed, consisting mostly of mobile silty-sandy sediments. Nevertheless, numerous submarine rocky substrates of biogenic concretions, called “grébeni” or “trezze” in the Gulf of Trieste and “tegnúe” off the coast of Venice, are irregularly scattered over the soft bottom of this Adriatic Sea sub-basin (Casellato and Stefanon, 2008; Ingrosso et al., 2018; Lipej et al., 2016). Their size ranges from a single small block of 1 m^2 up to a few 1000 m^2, and their height rarely exceeds 4 m. These rocky substrates are suitable for the settlement and development of specific floristic and faunistic assemblages, that are favoured by the accumulation of calcareous incrusting algae, creating complex biostructures commonly referred to as “coralligenous” and giving the colourful underwater landscape a typical appearance (Lipej et al., 2016; Turicchia et al., 2022).

For this reason, since 2015, a limited number of biogenic outcrops in the Gulf of Trieste have been legally protected under the European Habitats Directive (92/43/EEC) and included in the European Natura 2000 network as Sites of Community Importance (Decision EU 2015/69 of December 3, 2014) (Bettoso et al., 2023). These sites are generally called “IT3330009 - Trezze San Pietro e Bardelli” (Figure 2.2).

Up to 4000 outcrops are currently recorded in the Northern Adriatic Sea (Figure 2.1), mostly off the Venetian coast, while in the Gulf of Trieste about 250 have been mapped so far, most of them off the lagoon of Marano and Grado, at a distance of 3 to 10 nautical miles (nm) from the coast and at a depth ranging between 13 and 25 m (Caressa et al., 2001).

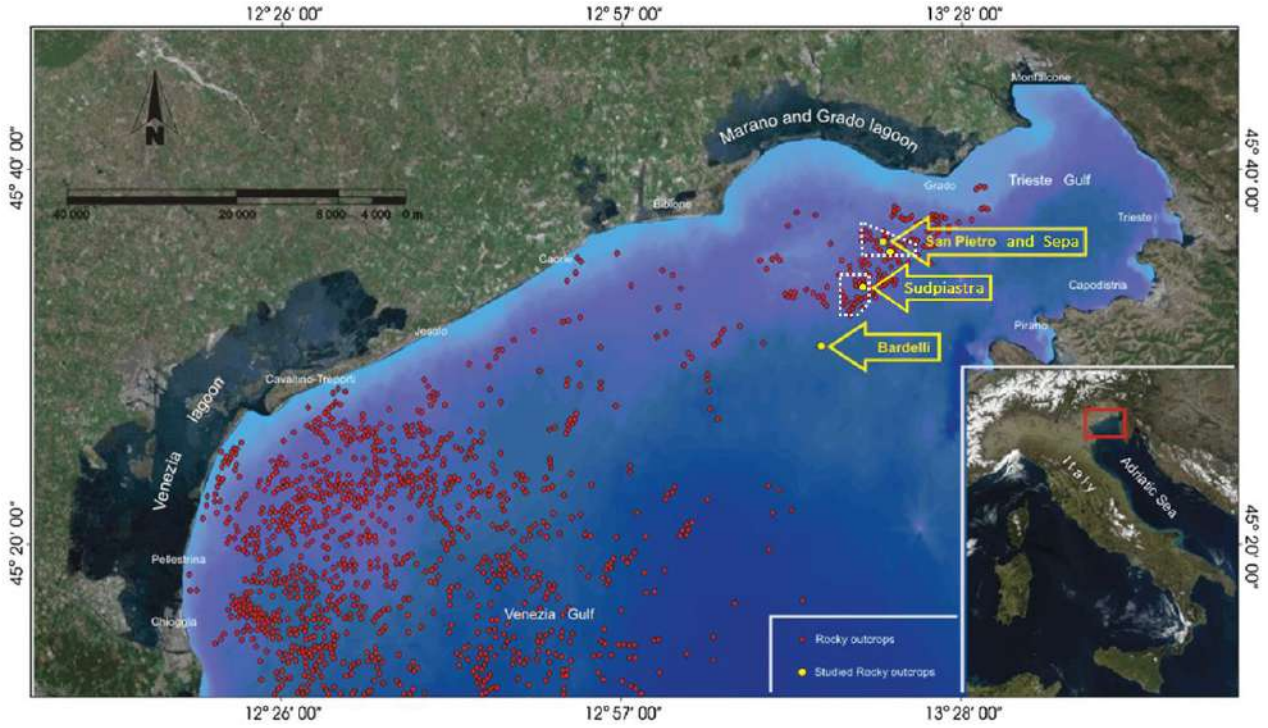

Figure 2.2. Location map of the northern Adriatic Sea rock outcrops (red dots) where the position of trezze San Pietro, Sepa, Sudpiastra and Bardelli is highlighted. Sites of Community Importance in the Gulf of Trieste are indicated by white dashed polygons (mod. from Gordini et al., 2012).

These coralligenous buildups are often associated with gas seeps, thus leading to interpret such deposits as methane-derived carbonates. In fact, several gas fields were discovered and exploited during the 1960s in the Northern Adriatic Sea, where, particularly in the averagely 22 m deep Gulf of Trieste, gas seeps can produce up to 20 m-high gas flares and intermittent bubbling within the water column (Donda et al., 2019; Gordini et al., 2012). These seep gases, mainly composed of CH_4 and occurring both in deep and shallow Plio-Quaternary successions, are microbial in origin and mostly originate from laterally persistent Late Pleistocene peat layers, which are widely distributed throughout the Northern Adriatic Sea and represent the main source of organic matter feeding the gases (Donda et al., 2019).

Figure 3.5. Hydrophone for acoustic measurements of noise radiated by the gas bubble oscillating walls.

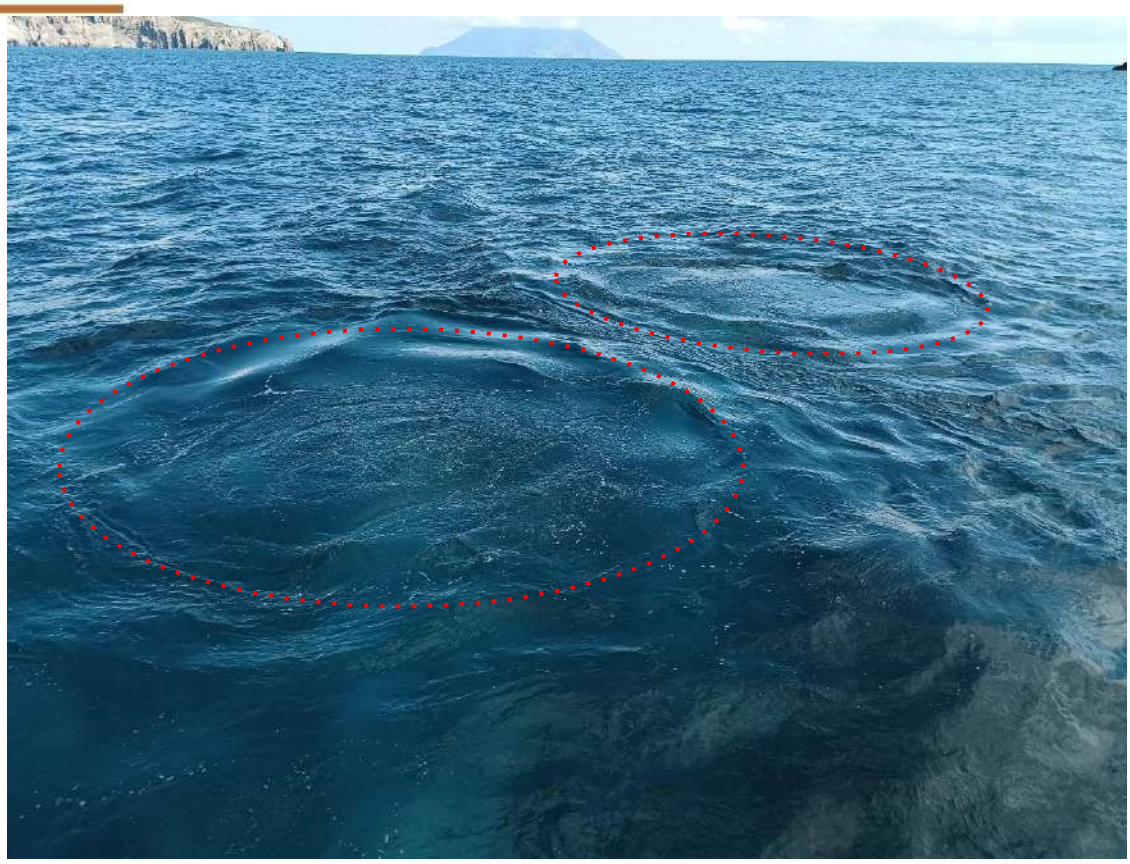

Figure 3.5. Bubble formation on the water surface due to hydrothermal vents in “Bottaro Twins”.

3. MATERIAL AND METHODS

3.1. Monitoring plan details

The four sampling campaigns foreseen by the MEFISTO project were carried out between March 2024 and April 2025. For Panarea island, the first campaign - under winter conditions - was completed between 21st and 23rd March 2024, while the second campaign, which aimed to capture a snapshot of the summer gas dynamics and environmental setting in the area, was conducted between September 26-28th 2024. Both campaigns have been carried out on board the M/N Corvo and thanks to the support of the Panarea Natlab Italy facility (operated by OGS).

Figure 3.1 Vessels supporting the project activities during the four MEFISTO campaigns: M/N Corvo (top) operating off Panarea island and M/N Castorino 2 (bottom) operating on the “trezze” off the Marano and Grado lagoon.

The campaigns in the “Trezze” of the Northern Adriatic Sea were carried out in July 2024 and April 2025, respectively. The first campaign, snapshotting the sites under summer conditions, was done between 16th and 18th July 2024, whereas the second campaign was conducted between April 7th-10th 2025, thus sampling the various sites during winter conditions. Both samplings were carried out with the logistic support of the M/N Castorino 2, Shoreline soc. cop. and the Grado Coast Guard.
From all the investigated sites, a sublist was selected as study cases for acoustic investigation, according to the information about gas seeping activity collected through a preliminary visual inspection performed by scuba divers. Full reports of the site selection procedures are available in MEFISTO Deliverable 1-3. The list of selected study areas with geographical coordinates is shown in table 3.1.

Table 3.1 - Main features of the stations investigated at both Southern Tyrrhenian Sea and Northern Adriatic Sea sites, in the framework of the MEFISTO project.

Area	*Station*	*Depth (m)*	*Longitude (Degree Minutes)*	*Latitude (Degree Minutes)*
Panarea - Southern Tyrrhenian Sea	Black Point Bubbling	21.0	15°06.630' E	38°38.217' N
Panarea - Southern Tyrrhenian Sea	Bottaro Twins	6.25	15°06.623' E	38°38.324' N
Panarea - Southern Tyrrhenian Sea	Hot/Cold1	10.0	15°04.704' E	38°38.553' N
Trezze - Northern Adriatic Sea	San Pietro	14.0	13°20.276 E	45°36.191 N
Trezze - Northern Adriatic Sea	Sepa	16.7	13°20.581 E	45°35.622 N
Trezze - Northern Adriatic Sea	Sudpiastra	19.0	13°18.305 E	45°33.218 N

3.2. Scientific Instrumentation Used

During the four MEFISTO campaigns, 10 sets of acoustic data were collected to attempt the tracking of degassing activity in the selected study sites. In order to accomplish this, proper sensors, able to record the underwater soundscape, were used. During all the campaigns (March 2024 and September 2024 in Panarea, July 2024 and April 2025 in North Adriatic "Trezze" sites) two Ocean Sonics IcListen digital hydrophones model SA9L were employed. Both instruments collected, digitised and stored audio frames with a frequency bandwidth of 12.8 kHz and a voltage sensitivity of -160 dBV re µPa. The underwater sensors were coupled with a metal pedestal, ensuring a stable deployment close to the selected bubble emissions. The bottom positioning was managed directly by scuba divers in order to properly select the ideal area on each site and evaluate the distance from the emission points, thus obtaining a well defined acoustic signal from the investigated seeps, avoiding at the time close proximity from the most energetic bubble streams that could saturate the acoustic intensity levels.

At each site, the smart sensor was configured to acquire continuously for ~10 hours 2-minute-long bursts of records of the sound radiated by the bubbles released by the vents. The setup also included the use of a rope in order to properly signal the sensor and guarantee an easy recovery, specifically in sparse and uniform underwater environments.

3.3. Acoustic procedure to estimate the gas flow

First of all, the acoustic data acquired were visually inspected in order to evaluate the superimposing effect of the noise and the quality of the sound received from the emissive sources.

For each site, the acoustic data were merged by the use of specific algorithms able to build-up a single time-coherent audio record, in order to have an overall view on the spectral features of the time-series. The visual inspection allowed us to identify the spectral bands corresponding to the acoustic signatures of individual bubble events and gas-jet streams and properly adapt the band-pass pre-filtering process to apply a first denoising. The identification of the different power spectral features was mandatory also to select the proper technique to estimate the size distribution of the bubble population emitted by each site in turn, thus proceeding to quantify the flux emitted [Leifer 2010, Leighton 2007].

The concept behind the use of the acoustic methods to passively identify and estimate the gas output from an underwater source lies in the mechanisms of the ascending gases from a nozzle [Ross 1976, Little et al. 1990, Crone et al. 2006]. The rapid collapse of the gas "neck" connecting the bubble to its source triggers a volumetric oscillation at a fundamental frequency, also defined as natural frequency or **breathing mode** [Minnaert 1933, Strasberg 1976, Leighton 1994]. This oscillation radiates a transient acoustic signal, which can be modeled as an exponentially decaying sinusoid.

3.3.1. High and persistent fluxes

In persistent fluxes, where the individual bubble pulses often overlap, it is not possible to identify a single bubble acoustic event and count one by one [Leighton 1994, Bergés et al. 2015]; therefore, a spectral approach is adopted [Roche et al. 2022, Leighton and White 2011]. Thus, the Power Spectral Density (PSD) is analysed and the total recorded spectrum S(ω) is considered the incoherent sum of the energy spectral densities of all individual bubbles produced

$$S(\omega) \approx \int_0^\infty D(R_0)|P(\omega, R_0)|^2 dR_0$$

where $D(R_0)$ is the Bubble Size Distribution (BSD) - the number of bubbles generated per second for a given radius R_0 and $|P(\omega, R_0)|^2$ is the theoretical pressure power spectrum of a single bubble of that size. Once the BSD ($D(R_0)$) is obtained from the inversion of the previous equation, the developed algorithm calculates the total gas flow rate (Q) by integrating the volume of all bubbles produced per unit of time:

$$Q = \int D(R_0)\left(\frac{4}{3}\Pi R_0^3\right) dR_0$$

This result provides the gas flow emission rate at the seafloor pressure.

3.3.2. Low and discontinuous fluxes

For low flux environments - where gas release is characterized by discrete, intermittent events rather than continuous plumes - the inversion approach shifts from a statistical spectral analysis to a deterministic "counting and sizing" strategy [Chad et al. 2011, Nikolovska and Waldmann 2006, Leifer and Tang 2007], often referred to as the Acoustic Bubble Signature Method. In these scenarios, the algorithm operates by isolating individual acoustic transients produced during the pinch-off of single bubbles.

At first, the individual acoustic pulses within the time-domain record are identified. Unlike high-flux systems where signals are masked by overlap, low-flux signals appear as distinct, short-duration (typically milliseconds) exponentially decaying sinusoids. After a temporal segmentation, the

algorithm uses a Short Time Fourier Transform (STFT) to determine the peak frequencies and an energy-based threshold technique to segment these pulses from the ambient background noise. To improve the Signal to Noise Ratio (SNR) and the detection of bubble events even in noisy soundscapes, the technique is enhanced with the application of another bandwidth-based threshold. Coupling two adaptive thresholding techniques implies the selection of the most suited thresholds that maximise the bubble event detection with respect to the environmental noise [Longo et al. 2021, Li et al. 2021, Li et al. 2019]. Once the event is isolated, the algorithm extracts its natural frequency (bubble breathing mode oscillation). The collection of all events allows the creation of a BSD based on the actual count of bubbles within discrete size bins. Lastly, the total volumetric gas flow rate (Q) is calculated by the cumulative sum of the volumes of all the detected bubbles over the inspected period (T):

$$Q = \frac{1}{T}\sum_{i=1}^{N} \left(\frac{4}{3}\pi R_{0,i}^{3}\right)$$

Such a method is highly accurate for seeps where bubbles occur in clusters or at low repetition rates, as it avoids uncertainties associated with spectral overlap.

4. PRELIMINARY RESULTS

Preliminary results of the acquired acoustic data from the seafloor during the investigations of each emission site are presented below. Due to the presence of significant environmental noise, within the time series of low-flux seeps, an extensive post-processing phase was required. This refinement was essential to isolate the signal from the background noise in order to characterise the bubble signatures and ensure the accuracy of the estimates, consequently necessitating an allocation of man-hours beyond the initial projections.
Underwater photos and videos were taken by scuba divers using GoPro cameras, with the aim to further validate the bubble size and flux estimations obtained by the acoustic methods.

4.1. Hydrothermal Vent Area off Panarea island

4.1.1. Black Point sites

In the "Black Point Bubbling" site the surveys highlighted the existence of mixed high and medium flux seeps featured by persistent degassing regimes. The elected spot for the two campaigns exhibited a medium flux. The resulting average PSD (Fig. 4.1) of the whole acquired acoustic records highlights an emerging frequency peak relative to the bubbles emission centered at ~350 Hz with a less energetic peak centered slightly above the above mentioned one, at ~400Hz. Such an energetic peak was more intense in the first campaign rather than in the second. Being a persistent flux where overlapping bubbles are released, as confirmed also by the spectrograms (Fig. 4.2), the inversion algorithm based

on the spectral method was applied to determine the BSD and estimate the gas flow emission rate during the observing time-span.

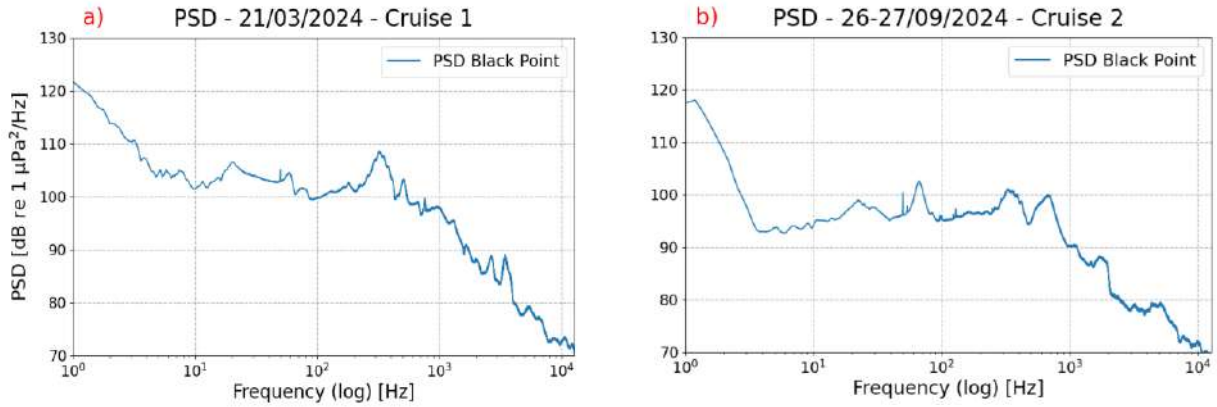

Figure 4.1 - Power Spectral Density related to *"Black Point Bubbling"* acoustic records acquired during Cruise 1 (a) and Cruise 2 (b).

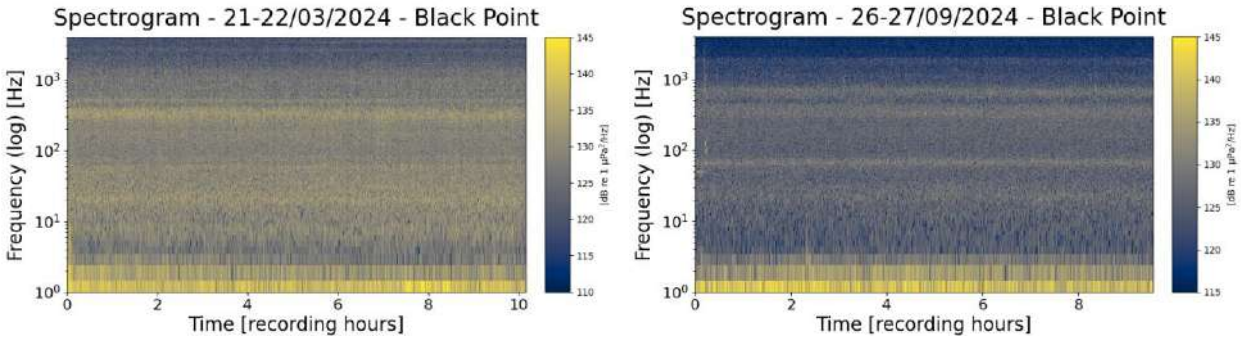

Figure 4.2 - Spectrograms referred to acoustic records acquired at the "*Black Point Bubbling*" site during Cruise 1 (left) and Cruise 2 (right).

The application of the inversion technique to the recorded spectrum allows us to retrieve the continuous temporal evolution of the flow emission rate for that site. The comparison between the two seasonal trends reveals a gas flow emission rate time series due to a turbulent gas release from the vent in both cases. However, the mean values of the inverted flow reach ~11.3 and ~6 l/min (see Fig. 4.3), respectively, highlighting a decrease in the degassing activity.

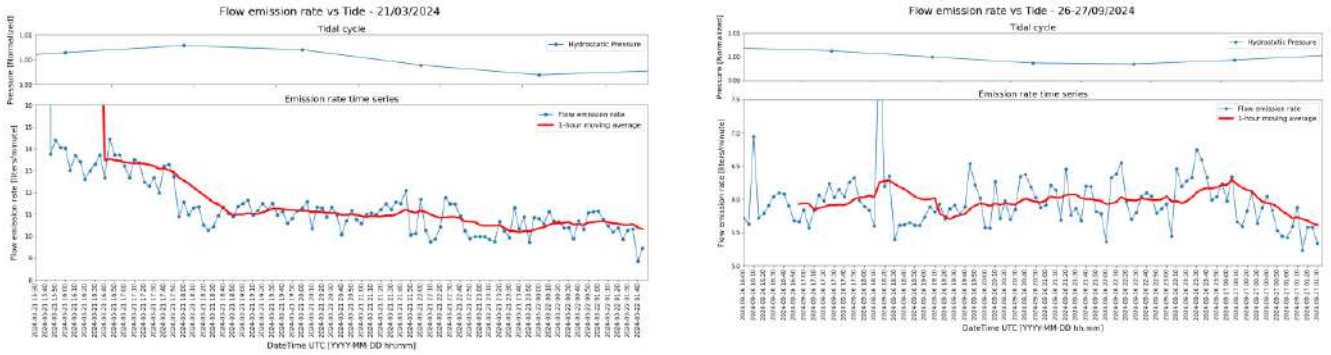

Figure 4.3 - a) Flux emission evolution over time estimation related to *"Black Point Bubbling"* acoustic records acquired during the Cruise 1 (left) and the Cruise 2 (right). The 1-hour-long averaged trend is described with the red line in each chart. Both temporal evolutions are compared with the tidal cycle (blue line graphs on top).

Figure 4.4. Hydrophone recording the noise radiated by the gas bubble oscillating walls in the "Black Point Bubbling" site.

4.1.2. Hot/Cold site

In "Hot/Cold1" area, the visual inspection of the site operated in diving displayed a low and intermittent emission degassing, in Cruise 1 and Cruise 2 as well. The persistence of such a pattern

was further confirmed by the acoustic records, as shown in Figure 4.6 a),b). Particularly, the site highlighted two major distributions, two centered between [1,1 - 0,7] and [0,4 - 0,3] mm, and one with a minor ascending rate located at upper bands and, thus, smaller radii located at 0,2 mm. Looking at the extracted time-series, it has been observed an interesting releasing schema, composed of slightly silent phases, quite regular, followed by a release of bursts of solitaire bubble clusters, with an emission rate of 5-10 ms each (see Fig. 4.8). Such a phenomenon may be ascribed to an accumulation mechanism happening in the shallower portion of the sandy bottom, where the energy of solitary bubbles to overcome the hydrostatic load needs to reach a certain threshold to allow the release. The preliminary comparison between the emission rate and the tidal cycle reveals an unexpected relationship as the general emission rate decreases with the decreasing of hydrostatic pressure, as shown in Figure 4.9. Such behaviour could be ascribed to the presence of biological noise at the upper portion of the frequency band, whose spectral contents mimic the bubble characteristics, altering the general trend. A further refinement in the identification process, including a Time-domain validation is ongoing to better exclude spectral artifacts and provide a higher-quality BSD, thus enabling a finer temporal analysis of the phenomenon.

Figure 4.5. The INGV hydrophone deployed in one of the hot patch detected in “Hot/Cold1”, in the proximity of a not-stationary bubble seep. Diver pursuing sampling activities in the background.

The analysis of the spectral content of the audio records collected in both periods shows the presence of a main peak likely due to bubble emission in the frequency range from ~400 to ~4000 Hz. Comparing the energetic levels extracted from the audio records, similarly to “Black Point bubbling” site, a weaker degassing activity is recorded during the Cruise 2.

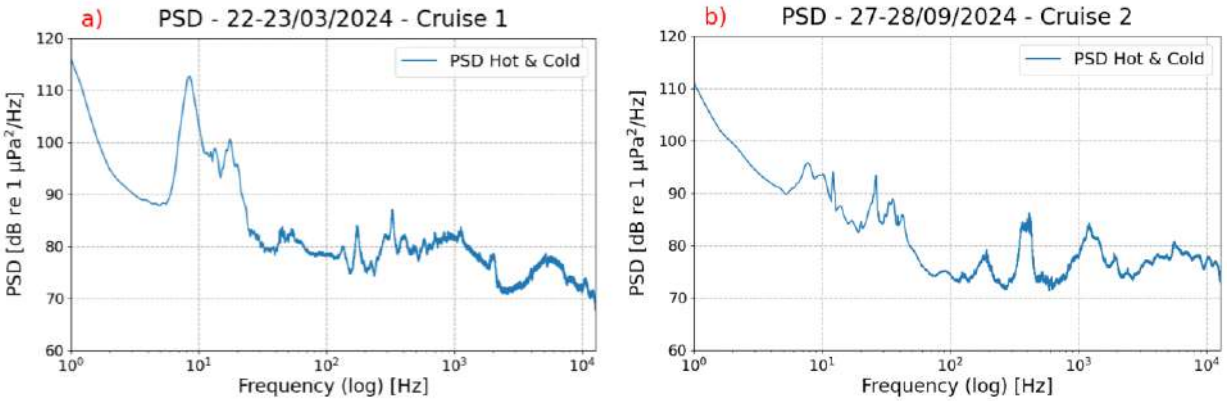

Figure 4.6 - Power Spectral Density related to the *"Hot/Cold"* acoustic records acquired during the Cruise 1 (a) and the Cruise 2 (b).

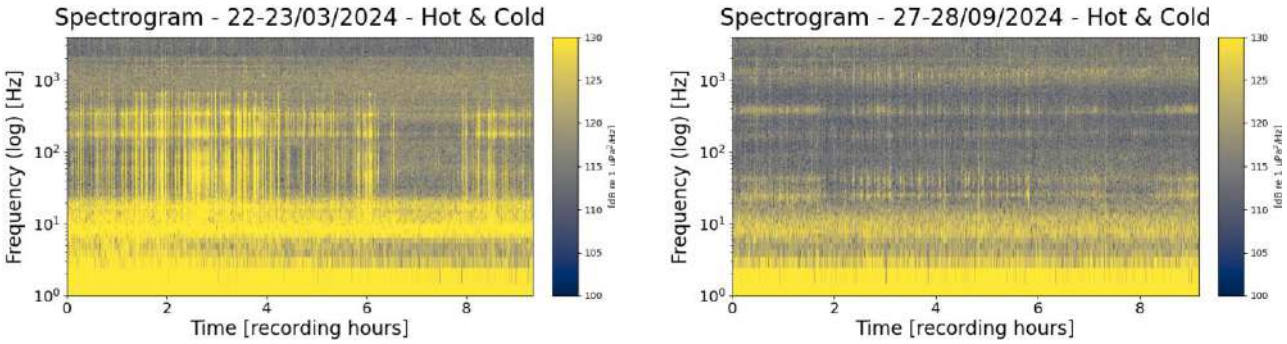

Figure 4.7 - Spectrograms related to the *"Hot/Cold"* acoustic records acquired during the Cruise 1 (left) and the Cruise 2 (right). The vertical line in light yellow (right) represents instrumental noise due to the signalling rope attached to the pedestal

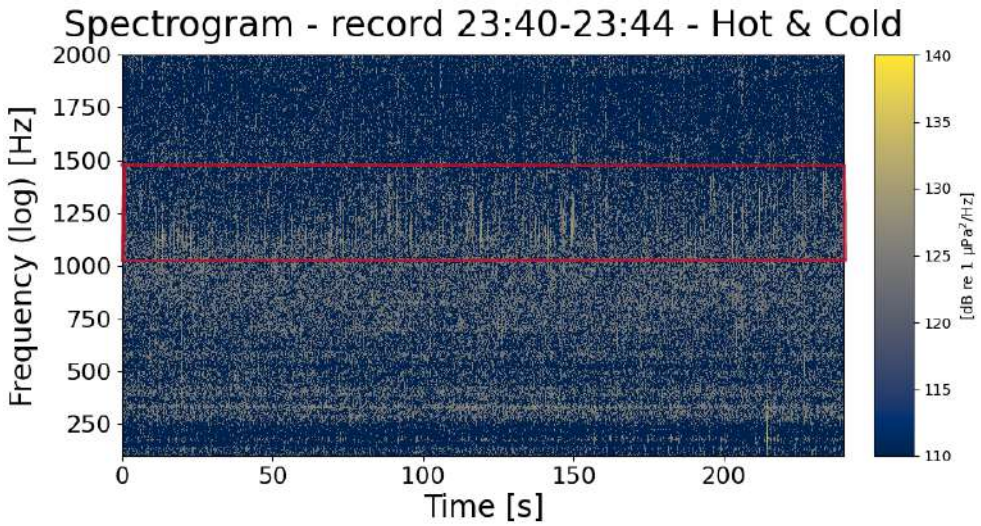

Figure 4.8 - Spectrograms related to 2 consecutive 2-minute-long audio frames from Cruise 1 characterized by a bubble cluster release.

Through the application of the Acoustic Bubble Signature Method, a distribution of bubble sizes was identified and extracted, confirming the less amount of bubbles emitted with respect to the previous acquisition.

a)

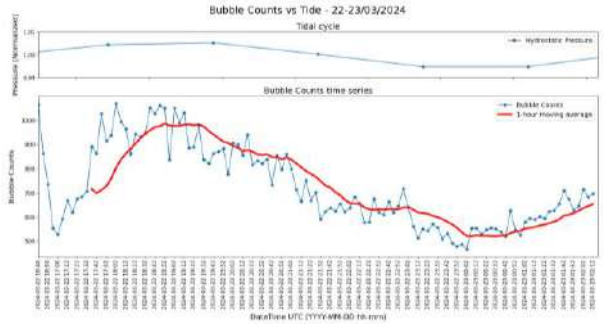

b)

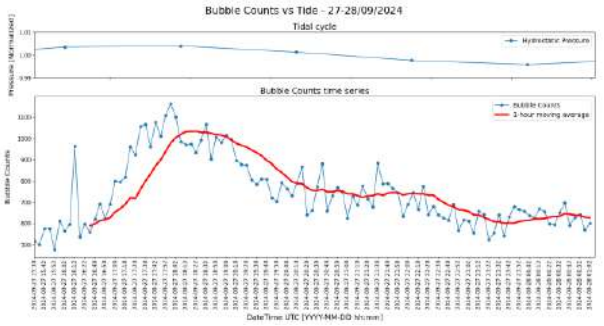

Figure 4.9 - a) Bubble event counts evolution over time related to *"Hot and Cold 1"* acoustic records acquired during the Cruise 1 (left) and the Cruise 2 (right). The 1-hour-long averaged trend is described with the red line in each chart. Both temporal evolutions are compared with the tidal cycle (blue line graphs on top).

4.1.3. Bottaro sites

The Bottaro study area is characterized by the presence of persistent high flux emissions from three main submarine vents. Among these, two are identified as “Bottaro Twin” and the other one as “Bottaro Single”, according to their spatial position. They show very intense bubbling activity forming uprising plumes featured by multiple overlapping between bubbles which are not distinguishable from each other, as confirmed by both site investigations and inspection of acoustic records. Hydrophone was deployed to acquire data close to the “Bottaro Twin” station (see Fig. 4.15).

The analysis of the acoustic energy levels shows spectral components likely due to bubble formation at the vent in the frequency range from ~100 Hz up to 2000-2500 Hz, in each data series.
As well as the “Black Point bubbling” study area, the application of the inversion modelling algorithm based on a spectral approach allowed us to estimate the evolution over time of the flow emission rate. In this case, the comparison between acoustic data acquired during both Cruises showed quite similar energetic levels, albeit data from Cruise 1 present more intense signals at low frequencies (<100 Hz), as visible in the spectrograms (see Fig. 4.13). The application of the acoustic inversion model provides a mean value of total gas flow emission rate equal to 33.5 and 36.32 l/min, respectively. It is also worth noting that results obtained for this specific case may be affected by underestimation, as the multiple bubbles overlapping could inhibit the capability of the algorithm in the detection of a very large number of simultaneously emitted bubbles.

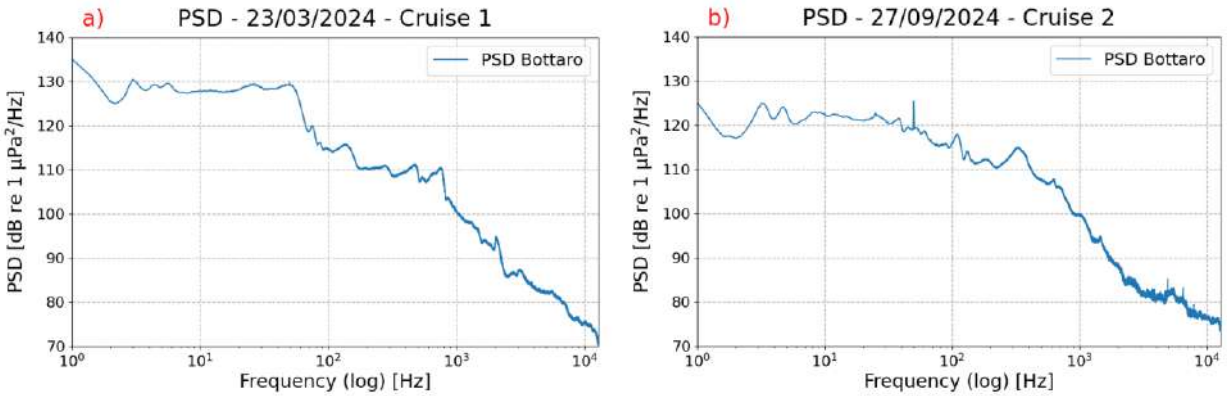

Figure 4.10 - Power Spectral Density related to the *“Bottaro”* acoustic records acquired during the Cruise 1 (a) and the Cruise 2 (b).

a) b)

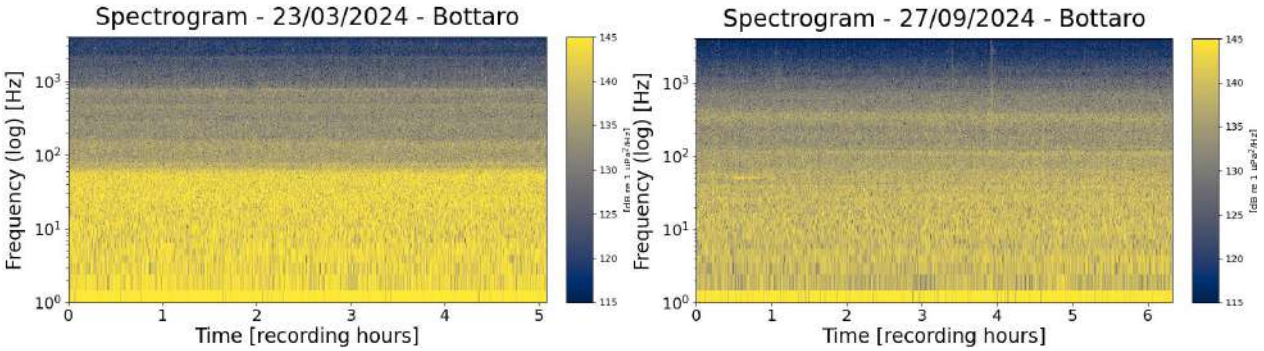

Figure 4.11 - Spectrograms related to the *"Bottaro"* acoustic records acquired during the Cruise 1 (a) and the Cruise 2 (b).

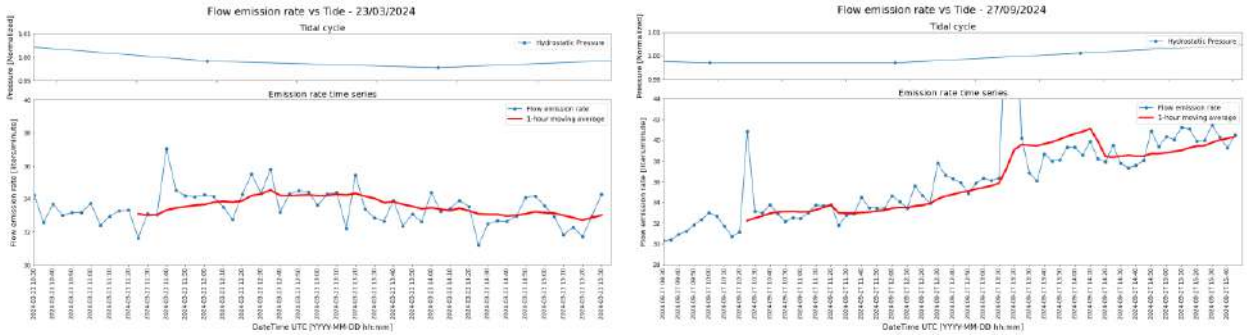

Figure 4.12 - a) Flux emission evolution over time estimation related to *"Bottaro Twin"* acoustic records acquired during Cruise 1 (left) and Cruise 2 (right). The 1-hour-long averaged trend is described with the red lines in each chart.

Figure 4.13. Hydrophone recording the noise radiated by the gas bubble oscillating walls in “Bottaro Twins” station.ora

4.2. Grébeni/Trezze/Tegnúe - Northern Adriatic Sea

4.2.1. SEPA site

SEPA site exhibited an intermittent degassing activity in the proximity of the coralligenous biogenic outcrops. Low emissions were observed in cruise 1 and cruise 2 as well, with a slight increase in the activity. The extent of the degassing area and the non-persistent position of active seeps limited the choice of deployment of the hydrophone, despite that, the acquired data and distance from the coast allowed to obtain a good quality of data. A total amount of ~10 hours of acoustic records were collected in both cruises. The visual inspection conducted in diving highlighted the release of solitary bubbles ranging between ~ [0.5-0.1] cm of radius. Considering the seabed depth and the gas content, by the Minnaert formula we attained a *fr* product of ~511 $Hz \times cm$.

The processing of the spectral signature of the audio records bounded between a larger interval of [400 - 6000] Hz, confirms the existence of bubbles mainly peaked at ~2200 Hz. The general distribution spans between [0.20 - 0.12] cm of radius, thus confirming the on-site observation. Some episodic larger bubbles were detected, peaking at ~500 Hz, suggesting a pocket-like accumulation process that may be driven by the geometry of the outcrops.

a) b)

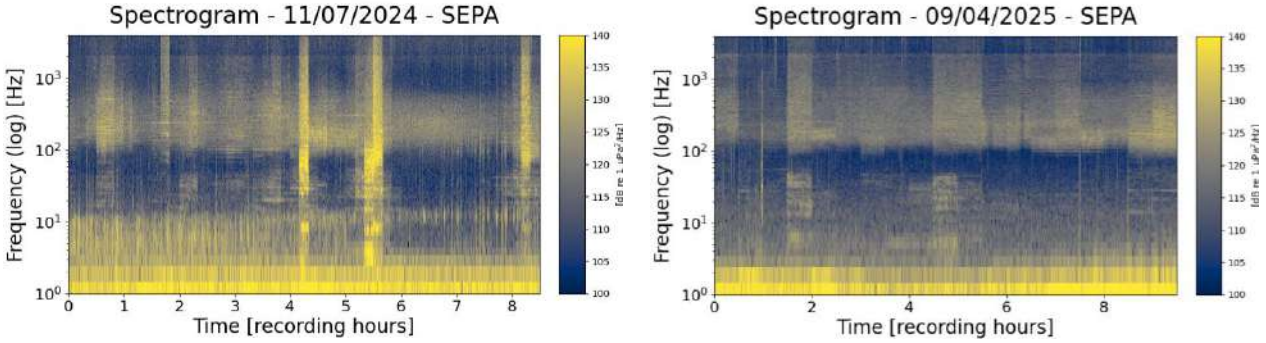

4.14 - Spectrogram related to the *"SEPA"* site acoustic records acquired during the Cruise 1 (a) and Cruise 2 (b) . The vertical line in light yellow (right) represents transient ship traffic noise.

More commonly, slightly silent phases, followed by a release of bursts of solitaire bubble clusters were detected. Such a phenomenon, similarly to those observed in Panarea "Hot and Cold 1" site, may be ascribed to the same accumulation mechanism happening in the shallower portion of the sandy bottom, where the gas trapped beneath the seabed needs to reach a certain amount to overcome the hydrostatic load and being released.

The comparison between acoustic data acquired during both Cruises shows a slight increase in the amount of tracked escaping bubbles events (see Fig. 4.18). Both time-series display a tidal modulated emission rate, which seems to be more empathised in the second Cruise, where a relative tidal minimum is reached. The application of the inversion model provides a cumulative released volume of gas equal to 0.48 and 3.8 litres over 10 hours, respectively. Such estimation could however be slightly affected by limitation in the detection due to the extension of the degassing site, as the emissions sourced at long distances from the hydrophone may be attenuated and hidden under the environmental soundscape. In contrast, a certain number of false detected events due to the presence of ship traffic and biological noise inhibits the capability of the algorithm in the detection of bubble events.

The implementation of a Time-domain validation process will better exclude spectral artifacts and provide a higher-quality BSD, enabling a finer temporal analysis of the phenomenon.

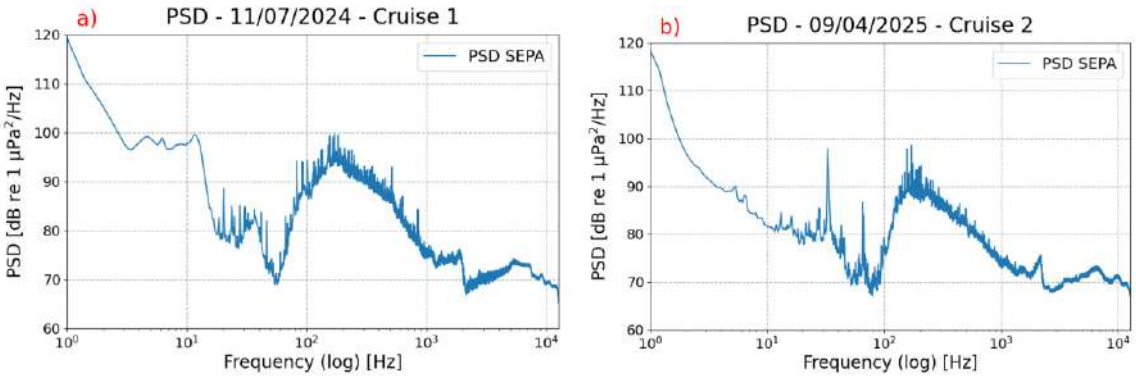

Figure 4.15 - Power Spectral Density related to the *"SEPA"* acoustic records acquired during the Cruise 1 (a) and the Cruise 2 (b).

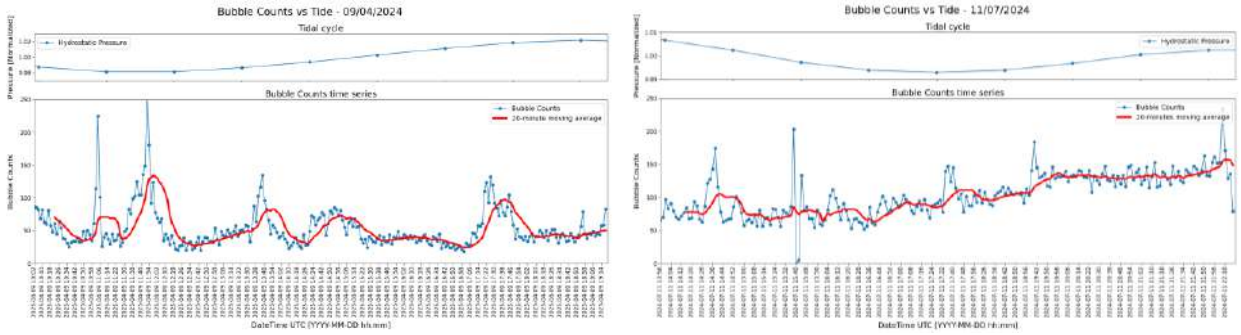

Figure 4.16 - a) Bubble event counts evolution over time related to *"SEPA"* acoustic records acquired during the Cruise 1 (left) and the Cruise 2 (right). The 20-minutes averaged trend is described with the red line in each chart. Both temporal evolutions are compared with the tidal cycle (blue line graphs on top).

Figure 4.17. The INGV hydrophone deployed close to the outcrops detected in "SEPA" site, in the proximity of an intermittent bubble seep.

4.2.2. San Pietro site

In the "San Pietro" area, the visual inspection of the site operated in diving displayed an extremely low and rather absence of activity emission degassing in the proximity of the coralligenous biogenic outcrops. Discontinuous seeps spanned over a large area, and the choice of the proper spot to deploy the hydrophone was tricky. The acquisition of acoustic records in this site was affected by battery-related issues that limited the length of data recorded. A total amount of ~3 hours of continuous recording were collected during the Cruise 2 (see spectrogram of Fig. 4.18 panel b)), but limited events were recorded. Nonetheless, a few bubble events, between [500 -2500] Hz were detected, with peaks centered mostly at ~900, ~2000 and ~2200 Hz. An accumulation mechanism with the subsequent burst release was observed as well, characterised by a less abundant number of bubbles, as shown in Fig. 4.19.

Considering the seabed depth and the gas content, by the Minnaert equation we attained a *fr* product of ~484 $Hz \times cm$. Consequently, the BSD related to the site was estimated to be within [0.95 - 0.22] cm of radius.

Applying the inversion model yields a cumulative gas release volume of 0.33 litres over 3 hours in the inspected area. It is worth noting that the same limitations that affected the previous sites are also valid for this estimation.

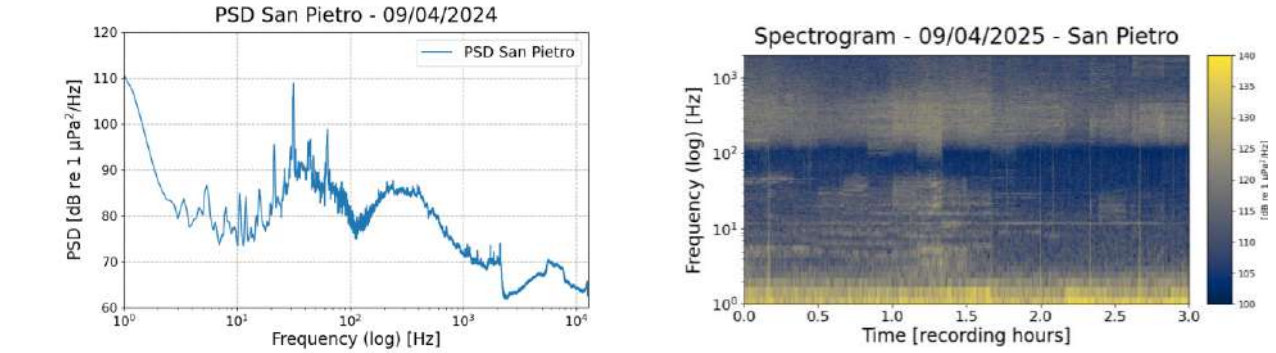

Figure 4.18 - Power Spectral Density (a) and Spectrogram (b) referred to the *"San Pietro"* acoustic records acquired during the Cruise 2.

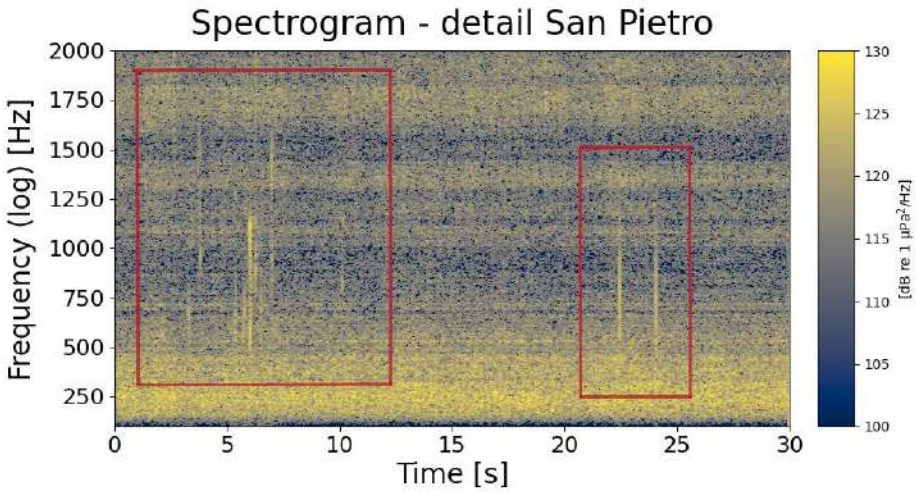

Figure 4.19 - Spectrograms detail extracted from a 2-minute-long audio frame from Cruise 2, characterized by a bubble cluster release at the "*San Pietro*" site.

Figure 4.20. Hydrophone recording the noise radiated by the gas bubble oscillating walls in the "San Pietro" station.

4.2.3. Sudpiastra site

Sud Piastra was characterised by very intermittent and sparse degassing activity. The hydrophone was deployed during cruise 2 at a depth of 19.0 meters. However, due to sea-state condition and environmental noise overlapping the frequency ranges related to bubbles' spectral contents no statistically significant data were collected (see spectrogram of Fig. 4.21 panel b).

a) b)

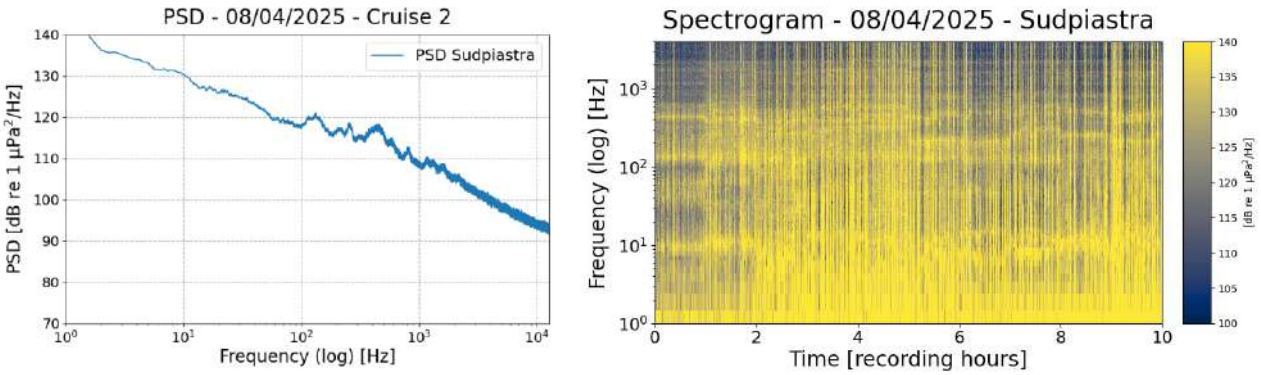

Figure 4.21 - a) Power Spectral Density related to the *"Sudpiastra"* site acoustic records acquired during the Cruise 2, where overlapping noise is hiding the emission spectral features. b) Spectrograms related to the *"Sud Piastra"* acoustic records acquired during the Cruise 2

MISSIONE 4
ISTRUZIONE
RICERCA

5. ACKNOWLEDGEMENTS

The MEFISTO research team would like to acknowledge the European Union that financially supported the project through the "Fund for the National Research Programme and Research Projects of Significant National Interest (PRIN)" in the framework of the NRRP - Next Generation EU Mission 4 "Education and Research". Thanks goes to Captain Angelo Portelli for the logistical support provided by the M/N Corvo vessel and crew during the activities conducted at sea. Special thanks goes to Dr. Valentina Esposito, Dr. Marco Graziano and Giuseppe De Rosa from OGS ECCSEL NatLab-Italy, who granted access to the facility and enthusiastically supported the onshore laboratory activities.

6. REFERENCES

Anzidei, M. and Esposito, A. (2003). New insights from high resolution bathymetric surveys in the Panarea volcanic complex (Aeolian Islands, Italy). In EGS-AGU-EUG Joint Assembly (p. 5923). http://www.cosis.net/abstracts/EAE03/05923/EAE03-J-05923.pdf

Anzidei, M. et al. (2005). The high resolution bathymetric map of the exhalative area of Panarea (Aeolian Islands, Italy). Annals of Geophysics. https://doi.org/10.4401/ag-3242

Bergès B.J.P. et al. (2015). Passive acoustic quantification of gas fluxes during controlled gas release experiments. International Journal of Greenhouse Gas Control, 38:64–79, July 2015. https://doi.org/10.1016/j.ijggc.2015.02.008

Boles, J. R. et al. (2001). Temporal variation in natural methane seep rate due to tides, Coal Oil Point area, California. Journal of Geophysical Research: Oceans, 106(C11), 27077-27086. https://doi.org/10.1029/2000JC000774

Calanchi, N. et al. (1999). Explanatory notes to the geological map (1: 10,000) of Panarea and Basiluzzo islands (Aeolian arc, Italy). Acta Vulcanologica, 11(2), 223-243.

Caliro, S. et al. (2004). Evidence of a recent input of magmatic gases into the quiescent volcanic edifice of Panarea, Aeolian Islands, Italy. Geophysical Research Letters, 31(7). L07619. https://doi.org/10.1029/2003GL019359

Capaccioni, B. et al. (2005). The November 2002 degassing event at Panarea Island (Italy): five months of geochemical monitoring. Annals of Geophysics. http://hdl.handle.net/2122/936

Caracausi, A. et al. (2005). Changes in fluid geochemistry and physico-chemical conditions of geothermal systems caused by magmatic input: The recent abrupt outgassing off the island of Panarea (Aeolian Islands, Italy). Geochimica et Cosmochimica Acta, 69(12), 3045-3059. https://doi.org/10.1016/j.gca.2005.02.011

Chad A. et al. (2011). Laboratory investigation of a passive acoustic method for measurement of underwater gas seep ebullition. The Journal of the Acoustical Society of America, 131(1):EL61–EL66. https://doi.org/10.1121/1.3670590

Ciais, P. et al. (2014). Carbon and other biogeochemical cycles. In Climate Change 2013: The Physical Science Basis. Contribution of Working Group I to the Fifth Assessment Report of the Intergovernmental Panel on Climate Change Change (pp. 465-570). Cambridge University Press.

Crone T.J. wt al. (2006). The sound generated by mid-ocean ridge black smoker hydrothermal vents. PLoS ONE, 1(1):e133, December 2006.https://doi.org/10.1371/journal.pone.0000133

De Astis, G. et al. (2003). Geodynamic significance of the Aeolian volcanism (Southern Tyrrhenian Sea, Italy) in light of structural, seismological, and geochemical data. Tectonics, 22(4). https://doi.org/10.1029/2003TC001506

Di Bella et al. (2022). Potential resilience to ocean acidification of benthic foraminifers living in Posidonia oceanica Meadows: The case of the shallow venting site of Panarea. Geosciences, 12(5), 184. https://doi.org/10.3390/geosciences12050184

Dolfi, D. et al. (2007). Dome growth rates, eruption frequency and assessment of volcanic hazard: Insights from new U/Th dating of the Panarea and Basiluzzo dome lavas and pyroclastics, Aeolian Islands, Italy. Quaternary International, 162, 182-194. https://doi.org/10.1016/j.quaint.2006.05.035

Leifer I. and Tang D. (2007). The acoustic signature of marine seep bubbles. The Journal of the Acoustical Society of America, 121(1):EL35–EL40. https://doi.org/10.1121/1.2401227

Leifer I. (2010). Characteristics and scaling of bubble plumes from marine hydrocarbon seepage in the coal oil point seep field. Journal of Geophysical Research: Oceans, 115(C11). https://doi.org/10.1029/2009JC005844

Leighton T.G. (1994). The Acoustic Bubble. Elsevier.

Leighton T.G. (2007). Theory for acoustic propagation in marine sediment containing gas bubbles which may pulsate in a non-stationary nonlinear manner. Geophysical Research Letters, 34(17). https://doi.org/10.1029/2007GL030803

Leighton T.G. and White P.R. (2012). Quantification of undersea gas leaks from carbon capture and storage facilities, from pipelines and from methane seeps, by their acoustic emissions. Proceedings of the Royal Society A: Mathematical, Physical and Engineering Sciences, 468(2138):485–510. https://doi.org/10.1098/rspa.2011.0221

Li J. et al (2019). A noise impact assessment model for passive acoustic measurements of seabed gas fluxes. Ocean Engineering, 183:294–304. https://doi.org/10.1016/j.oceaneng.2019.03.046

Li J. et al (2021). Acoustic and optical determination of bubble size distributions – quantification of seabed gas emissions. International Journal of Greenhouse Gas Control, 108:103313. https://doi.org/10.1016/j.ijggc.2021.103313

Little S.A. et al. (1990). The sound field near hydrothermal vents on axial seamount, juan de fuca ridge. Journal of Geophysical Research: Solid Earth, 95(B8):12927–12945. https://doi.org/10.1029/JB095iB08p12927

Longo et al. (2021). Black sea methane flares from the seafloor: Tracking outgassing by using passive acoustics. Frontiers in Earth Science, 9. https://doi.org/10.3389/feart.2021.678834

McGinnis, D.F. et al. (2006). Fate of rising methane bubbles in stratified waters: How much methane reaches the atmosphere?. Journal of Geophysical Research: Oceans, 111(C9). https://doi.org/10.1029/2005JC003183

Minnaert M. (1933). XVI.On musical air-bubbles and the sounds of running water. The London, Edinburgh, and Dublin Philosophical Magazine and Journal of Science, 16, 235-248. https://doi.org/10.1080/14786443309462277

Nikolovska A. and Waldmann (2006). Passive acoustic quantification of underwater gas seepage. In OCEANS 2006. IEEE. https://doi.org/10.1109/OCEANS.2006.306926

Roche B. et al. (2022). Methods of acoustic gas flux inversion—investigation into the initial amplitude of bubble excitation. The Journal of the Acoustical Society of America, 152(2):799–806, August 2022. https://doi.org/10.1121/10.0013220

Romano, D. et al. (2019). Hazard scenarios related to submarine volcanic-hydrothermal activity and advanced monitoring strategies: A study case from the panarea volcanic group (aeolian islands, italy). Geofluids, 2019, 1-15. https://doi.org/10.1155/2019/8728720

Ross D. (1976). Mechanics of underwater noise. Pergamon Press, New York.

Strasberg M. (1956). Gas bubbles as sources of sound in liquids. The Journal of the Acoustical Society of America, 28(1):20–26. https://doi.org/10.1121/1.1908212

Tassi et al. (2009). Low-pH waters discharging from submarine vents at Panarea Island (Aeolian Islands, southern Italy) after the 2002 gas blast: Origin of hydrothermal fluids and implications for volcanic surveillance. Applied Geochemistry, 24(2), 246-254. https://doi.org/10.1016/j.apgeochem.2008.11.015